Catalytic Mechanism of Class A β-Lactamase: Role of Lysine 73 and C3-Carboxyl Group of the Substrate Pen G in the Deacylation Step

Yasuyuki Fujii,* Masayuki Hata, Tyuji Hoshino, and Minoru Tsuda

Laboratory of Physical Chemistry, Graduate School of Pharmaceutical Sciences, Chiba University, 1-33 Yayoi-cho, Inage-ku, Chiba 263-8522, Japan

Received: June 12, 2002

The deacylation mechanism in hydrolysis of β-lactam antibiotics by class A β-lactamase was investigated by the density functional theory. The model compound was composed of a substrate penicillin G, four catalytic residues(Ser70, Lys73, Ser130, and Glu166), and a water molecule. We have found that the deacylation reaction proceeds via four elementary reactions. First, Lys73 is deprotonated by a concerted double proton transfer from Lys73Nζ to Ser130Oγ and from Ser130Oγ to C3-carboxylate in the substrate. Second, the acyl-enzyme tetrahedral intermediate (TI) is formed by an assistance of Glu166 which acts as a general base catalyst. Third, Lys73 is protonated by concerted double proton transfer from C3-carboxylic acid to Ser130Oγ and from Ser130Oγ to Lys73Nζ. Finally, the degraded substrate is detached from the enzyme in concert with a single proton transfer from Lys73Nζ to Ser70Oγ. It is remarkably noted that the deacylation is not proceeded only by Glu166, but Lys73 also participates in the reaction. Moreover, it has been found that the presence of the C3-carboxyl group of the substrate reduces the barrier height at the TI formation. This result suggests that the deacylation is a substrate-assisted catalytic process.

1. Introduction

β-Lactamases are produced by pathogenic bacterium and are serious enzymes to cause the resistance to β-lactam antibiotics. β-Lactamases deteriorate the pharmacological effect of β-lactam antibiotics by catalyzing the hydrolysis of the amide bond of the β-lactam ring. On the basis of the active site structure, they are classified in two major types: serine and metallo β-lactamase. As is well-known, the catalytic mechanism of serine β-lactamase involves acylation and deacylation. The acylation mechanism has been explored by much experimental and theoretical work, and the acylation is common to serine β-lactamase and the penicillin binding protein (PBP). By contrast, the deacylation is restricted to serine β-lactamase. This means that the essence of antibiotic resistance by serine β-lactamase arises from the deacylation reaction. Hence, understanding of the reaction mechanism of the deacylation can be of great importance to develop novel β-lactam antibiotics and potent β-lactamase inhibitors.

Class A β-lactamase is commonly detected in clinical scene and belongs to serine β-lactamase.[1] In our earlier work, we have examined a formation mechanism of the acyl-enzyme tetrahedral intermediate (TI) in the catalytic deacylation process of class A β-lactamase.[2] A convincing mechanism had already been proposed; that is, Glu166 removes a proton from a water molecule in concert with the nucleophillic attack of the water oxygen on acyl- carbonyl carbon of substrate.[3−19] Our earlier work has reasonably given a theoretical justification to the mechanism. On inducing the detachment of the degraded substrate from the active site of the enzyme after the TI formation, three probable mechanisms have been reported as depicted in Scheme 1: (I) A proton migrates from the side chain carboxyl group of Glu166 to Ser70Oγ directly;[8,11] (II) A proton migrates from the carboxyl group of Glu166 to Ser70Oγ via an water molecule;[9,13,20,21] (III) A proton migrates from the protonated side chain ammonium group of Lys73 to Ser70Oγ directly.[2,22] This reaction is important to the regeneration of the enzymatic activity. However, there has been no clear evidence for any mechanism. In the present study, we will investigate the whole mechanism of the deacylation reaction involving the detachment of the degraded substrate.

We have determined the active site structure of the penicillin G(pen G)-class A β-lactamase acyl-enzyme intermediate (AEI) using the molecular dynamics (MD) calculation, because the AEI is the start of the deacylation reaction. In this study, we refer to this AEI structure as "MD-derived AEI". From the structure of the active site in the MD-derived AEI, it was assumed that the first-elementary reaction of the deacylation is a concerted double-proton transfer(PT) from Lys73Nζ to Ser130Oγ and from Ser130Oγ to C3-carboxylate of the substrate (see section 3.1.1). Nearly 40 years ago, Blow et al. proposed a concerted double-PT from Ser195Oγ to His57Nϵ2 and from His57Nδ1 to Asp102Oδ in the catalysis of chymotripsin.[23] This double PT mechanism has been referred to as a "charge relay system". The first-elementary reaction of the present work seemed to be similar to the charge relay system. However, the potential energy difference between the reactant and the product of the charge relay system is known to be unrealistically large ($\Delta E > 30$ kcal/mol), if the potential energies were calculated by simple *gas phase* quantum chemical (QC) calculation.[24−26] It is well-known that the problem arises from the neglect of the environmental effect on the active site.[27−30] Accordingly, gas-phase QC calculation is considered to be inadequate for verification of the proposed deacylation mechanism of the present study, because the mechanism involves the double-PT reaction. In this study, the self-consistent reaction field (SCRF) theory based on the Onsager model[31] was adopted to take into account the environmental effect inside a protein

* To whom correspondence should be addressed. E-mail: yfujii@p.chiba-u.ac.jp. Phone: +81-043-290-2927. Fax: +81-043-290-2925.

10.1021/jp021414c CCC: $22.00
Published on Web 08/21/2002

SCHEME 1

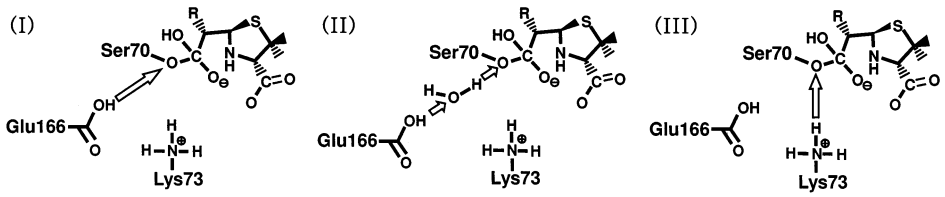

into the QC calculation. This SCRF theory was developed by[32] and implemented in the computational program by Wong et al.[33] Another SCRF theory developed by Tomasi[34] has been utilized in several studies for the same purpose.[35−37] The SCRF theory based on the Onsager model is more simple than the SCRF theory of Tomasi. The SCRF theory based on the Onsager model is easily applicable to the geometry optimization which is substantial to solve the reaction mechanism.[38]

The deacylation mechanism we addressed above depends on the C3-carboxyl group in pen G. Therefore, this enzymatic reaction is anticipated to be a substrate-assisted catalysis (SAC). According to Laws and Page, a pen G derivative that had an acethyl group at C3 was inadequate for the substrate of the enzyme.[39] Additionally, the derivative with a C3-amide group was found to be also inadequate substrate.[40] These studies indicated that the C3-carboxyl group in the substrate had a good potential to participate in the catalysis of the enzyme. To clarify if the deacylation mechanism is SAC or not, we also examined another deacylation path without the C3-carboxyl group.

2. Method

2.1. Construction of the Computational Model Compound. The structure of the AEI is hard to approach by experimental methods because of the deacylation activity of the enzyme. Chen and Hertzberg reported a crystal structure of an AEI analogue which composed of the class A β-lactamase from *Sthaphylococcus aureus* PC-1 and clavulanate moiety.[41] The three-dimensional structure of the AEI analogue was entered as 1BLC in the Protein Data Bank (PDB).[42,43] We constructed the AEI structure from this AEI analogue because this AEI analogue contained the wild-type enzyme (WTE) of class A β-lactamase and the catalytic deacylating water existed near the active site. To build the AEI structure from the 1BLC, energy minimizations and MD calculations were performed. These computations were executed with the program package AMBER4.1.[44] The united atom force field[45] was applied except for the degraded substrates (clavulanate or pen G) binding to Ser70 and several important residues (Lys73, Ser130, Asn132, Glu166, Lys234, and Gln237). For these important residues, the all-atom force field[46] was assigned. The amino group of the Lys73 side chain was protonated ($-N\zeta H_3^+$) by using this force field. This protonation was consistent with the result of a series of pK_a measurement studies.[18,19] The partial charges of the substrate bonding to Ser70 were determined by MOPAC PM3 calculation.[47] The solvent used was the TIP3P water model,[48] and nearly 4000 water molecules were generated by the Monte Carlo method.[44] The periodic box size was 67.5 Å × 54.7 Å × 47.4 Å. The MD simulations were performed starting from the energy-minimized structure. The energy minimization included the initial solvent relaxation and followed whole system relaxation. In the energy minimization on the whole system, the steepest descent methods were performed in early cycles and then the conjugate gradient methods were performed latter. The temperature of the whole system was gradually increased by heating from 5 to 310 K for the first 20 ps, and then it was kept at 310 K for the next 100 ps descent, and then the 5000 steps of the conjugate gradient method were executed. To simplify these calculation, the SHAKE procedure[49] was applied to constrain all of the bonds involving the hydrogen atom. The integration time step was 1.0 fs. van der Waals interactions were truncated at 15.0 Å. The Coulomb terms in the whole system were explicitly calculated without using a cutoff. The calculation of the coulomb terms was accelerated with a hardware accelerator, called MD-engine.[50]

Because the β-lactam ring and the adjacent five-membered ring of the clavulanate moiety had been cloven in the original PDB data, the inhibitor was restructured by closing the two rings, and a balanced structure was obtained by the MD calculation for 100 ps at 310 K. Next, the initial structure of the AEI was constructed by superimposing the β-lactam ring of pen G on that of clavulanate. The constructed AEI was fully stabilized by the MD calculation for 100 ps at 310 K, and the change in the distance of every hydrogen bond (we regarded a noncovalent bond below 3 Å as hydrogen bond) is not more than 0.1 Å during the 100 ps. The trajectory at that temperature (310 K for 100 ps) was considered to be the most probable structure under the physiologic condition, and the average structure in the 100 ps MD calculation was obtained. The active site structure of the AEI obtained is shown in Figure 1a. The model compound for QC calculation was constructed by extracting the atoms represented by open and closed circles on pen G, Ser70, Lys73, Glu166, and the deacylating water molecule (**Wat**), all of which were considered to be involved in the reaction. The atoms represented by closed circles were replaced with hydrogen atoms. The structure of the model compound is shown in Figure 1b.

2.2. Quantum Chemical Calculation. The electronic of the model compound was determined energy by density functional theory using the 6-31G** basis set. Becke's three parameter functional was used for the exchange term[51] and Lee−Yang−Parr's functional was used for the correlation term[52] (i.e., B3LYP/6-31G**). The transition state (TS) structure of each elementary reaction was determined by geometry optimization using the conjugate gradient method,[53] and it was confirmed by normal vibrational analysis that only one normal vibrational mode with an imaginary frequency appeared at the optimized TS structure. The steepest path on the potential energy hypersurface from the TS structure was computed in the forward and reverse directions of the normal vibrational mode corresponding to an imaginary frequency because the directions are theoretically verified to match the intrinsic reaction coordinate (IRC).[54] The minimum structures on the potential energy hypersurface, which are located at the last points of the steepest path, are the initial and final states of the reaction. In an actual enzyme, the movements of residues are restricted by other residues around them. The movement of carbonyl oxygen of pen G bonding to Ser70 is also restricted by the oxy-anion hole formed by two main-chain amide groups of Ser70 and Gln237.[7,55] To reflect this fact in the computational model, some atoms in the model compound were fixed to their initial positions through the QC

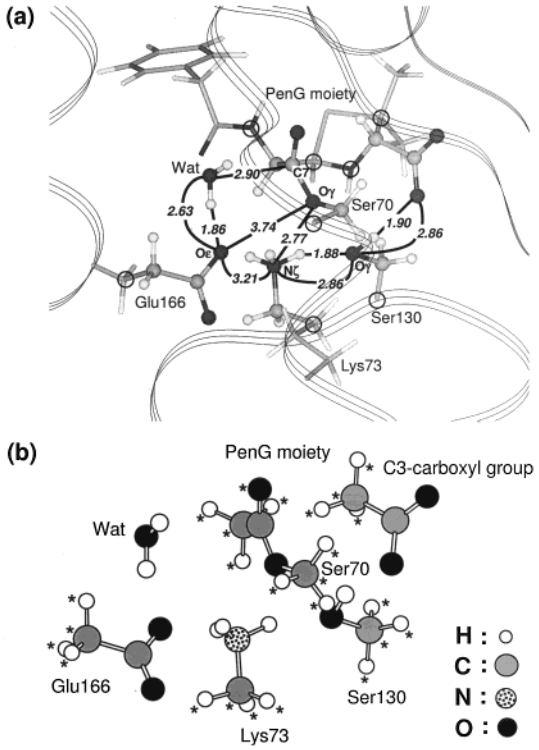

Figure 1. **(a)** Active site of pen G-bound AEI that obtained by MD calculation. **(b)** Initial model compound that used for the QM calculation to investigate the reaction mechanism of the deacylation. It consists of a acetate for Glu166 and a methylamine for Lys73 and a methanol for Ser130 and a methyl acetate for pen G moiety linked to Ser70 and a acetate for C3-carboxyl group of the substrate and a water molecule as a deacylating water.

calculation. The fixed atoms are shown by asterisks in Figure 1b. The SCRF theory used in this work was based on the Onsager reaction field model.[32,33] Because the active site of the enzyme is surrounded by other components of protein, it is desired to employ the SCRF theory for incorporating the environmental influence. According to the Onsager reaction field model, the model compound should be placed in a spherical cavity with radius a_0, surrounded by continuous medium with a dielectric constant ϵ.[31] Equation 1 represents the Kohn−Sham (KS) matrix elements of the model compound in the continuous medium:

$$\mathrm{KS}_{\mu\nu}^{\mathrm{rf}} = \mathrm{KS}_{\mu\nu} - \frac{2(\epsilon+1)}{(2\epsilon+1)}\frac{1}{a_0{}^3}\vec{\mu}\int \chi_\mu^* \hat{\mu}\chi_\nu \, \mathrm{d}r \qquad (1)$$

The environmental effects on the model compound correspond to the addition of an extra term to the KS matrix elements in a vacuum($\mathrm{KS}_{\mu\nu}$). $\vec{\mu}$ represents the molecular dipole moment operator of the model compound, $\hat{\mu}$ denotes the molecular dipole moment derived from the atomic charges of the model compound. χ indicates the basis set of the model compound. It was reported that dielectric constant ϵ of 20 was macroscopically appropriate for the investigation of a system which was surrounded by many ionized components in protein.[56−58] Therefore, the dielectric constant ϵ was set at 20. The radius a_0 was set at 5.48 Å determined from the volume of the model compound.

The computational program used was Gaussian 98.[59]

3. Results

3.1. Substrate-Dependent Deacylation Mechanism. It has been found from this work that the deacylation reaction consists of four elementary reactions. The potential energy profile is shown in Figure 2. The TS structures obtained are shown in Figure 3. The structures of energy minima appeard on the reaction path are shown in Figure 4, and its atomic distances which are important for reaction are listed in Table 1. The obtained mechanism is summarized in Scheme 2. The details for each elementary reaction are described in sections 3.1.1 to 3.1.4.

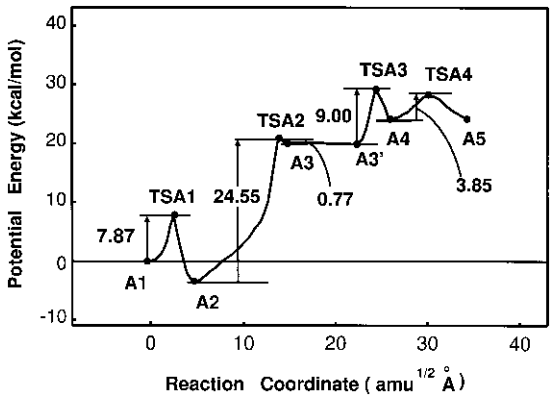

Figure 2. Potential energy profile for the substrate-dependent path. Horizontal and vertical axes represent the reaction coordinate along the steepest reaction path (amu$^{1/2}$ Å) and potential energy (kcal/mol), respectively.

TABLE 1: Important Atomic Distances for the Energy Minima along the Substrate-Dependent Path

atomic distances (Å)	A1	A2	A3	A3′	A4	A5
C7−Ow	3.13	3.12	1.57	1.61	1.58	1.43
C7−Ser70Oγ	1.37	1.36	1.50	1.49	1.53	1.85
Ow−Glu166Oϵ	2.69	2.68	2.62	2.79	2.79	2.96
Ser70Oγ−Glu166Oϵ	3.73	3.75	4.07	3.78	3.71	3.74
Ser70Oγ−Lys73Nζ	2.66	2.71	2.71	2.69	2.60	2.57
Lys73Nζ−Glu166Oϵ	2.74	3.11	3.20	3.20	2.97	2.96
Lys73Nζ−Ser130Oγ	2.89	2.76	2.70	2.70	2.67	2.75
Ser130Oγ−O_{C3}	2.61	2.65	2.64	2.64	2.64	2.70
Ha−Lys73Nζ	1.04	1.80	1.76	1.74	1.06	1.02
Ha−Ser130Oγ	1.91	1.00	1.00	1.02	1.64	1.89
Hb−Ser130Oγ	1.01	1.69	1.70	1.69	1.01	1.00
Hb−O_{C3}	1.64	1.00	1.00	1.00	1.71	1.77
Hc−Lys73Nζ	1.07	1.02	1.02	1.02	1.05	1.60
Hc−Ser70Oγ	2.56	2.17	1.87	1.89	1.79	1.03
Hw−Ow	0.99	1.00	1.68	1.89	1.93	2.19
Hw−Glu166Oϵ	1.71	1.68	1.01	0.99	0.99	0.97
Hw−Ser70Oγ	3.59	3.49	3.13	3.40	3.41	3.58

3.1.1. First Elementary Reaction. On our original anticipation, the first elementary reaction in the deacylation step had been presumed to be the formation of the TI. However, the active site structure in the MD-derived AEI depicted in Figure 1a indicated that Glu166 forms an ionic interaction with protonated Lys73. This state was thought to be unfavorable to the TI formation because the ionic interaction keeps Glu166 inactive for working as a general base to **Wat**. It was considered that the general base activity of Glu166 is enhanced by the deprotonation of Lys73. The feasible mechanism of the deprotonation of Lys73 was assumed to be a concerted double-proton transfer (PT) from Lys73Nζ to Ser130Oγ and from Ser130Oγ to C3-carboxyl oxygen (O_{C3}) in pen G because a hydrogen bond network among Lys73Nζ−Ser130Oγ−O_{C3} was formed in the MD-derived AEI. We successfully determined the transition state of this double-PT reaction **TSA1** from the initial model compound. This structure is theoretically obtained through geometry optimization to search a saddle point on the potential energy surface. It was confirmed by vibrational analysis that there appeared only one normal vibrational mode with an

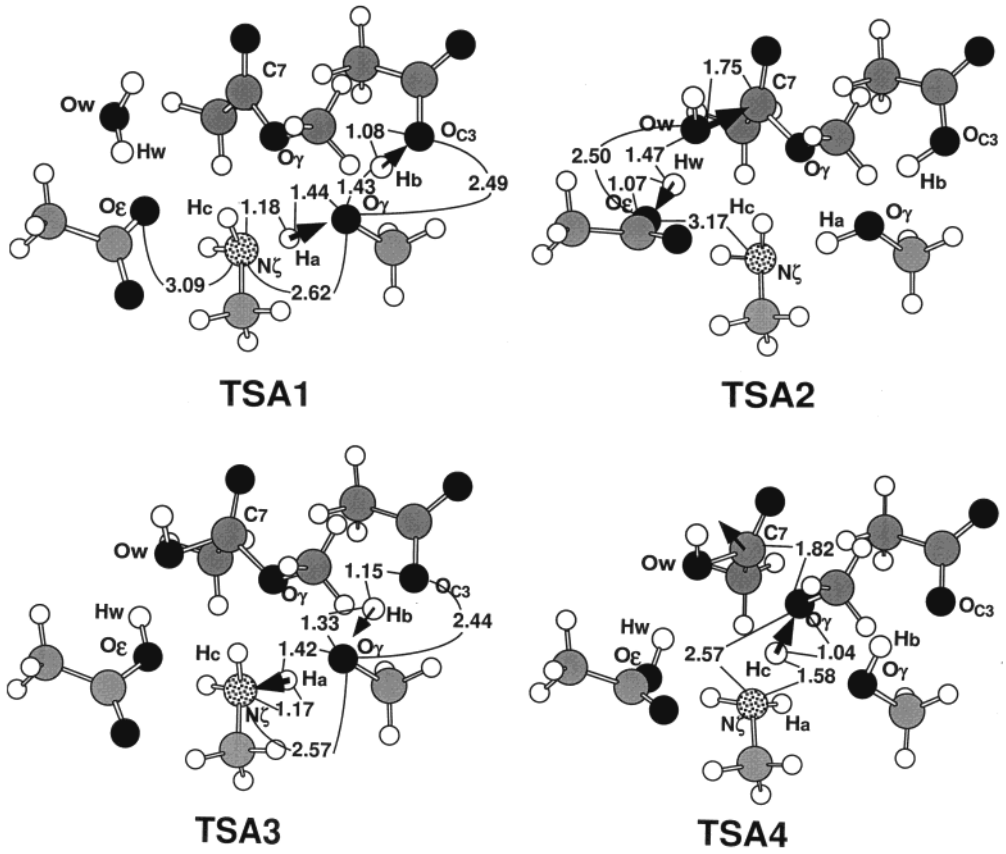

Figure 3. TS structures on the substrate-dependent path. Arrows represent the vibrational mode corresponding to an imaginary frequency which was obtained by vibrational analysis.

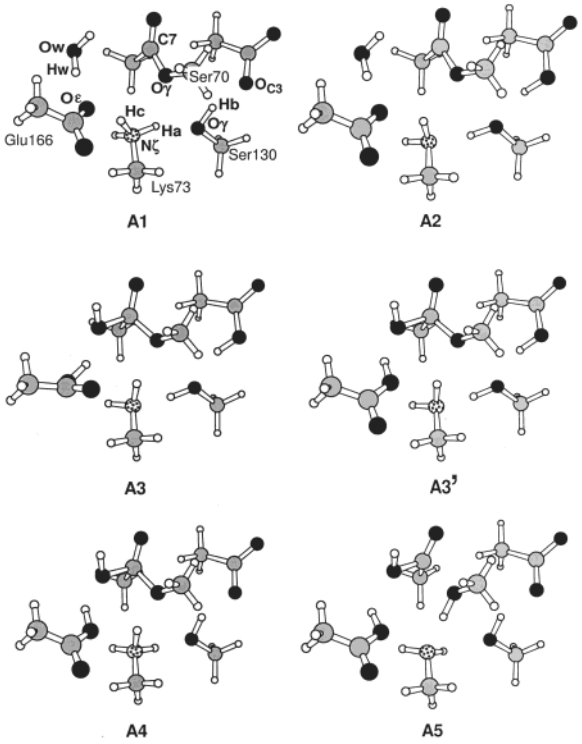

Figure 4. Structures of energy minima on substrate-dependent path.

imaginary frequency at the **TSA1** structure. In the largest atomic displacement seen in the vibrational mode, Ha from Lys73Nζ approached Ser130Oγ and Hb from Ser130Oγ approached O_{C3} in the second largest one. The distance between Lys73Nζ and Ser130Oγ was 2.62 Å. Ha−Lys73Nζ and Ha−Ser130Oγ distances were 1.18 and 1.44 Å, respectively. The O_{C3}−Ser130Oγ distance was 2.49 Å. Hb−Ser130Oγ and Hb−O_{C3} distances were 1.43 and 1.08 Å, respectively. It is important to confirm that the reactant structure obtained from **TSA1** corresponds to the active site structure in the MD-derived AEI. Hence, the steepest reaction path from **TSA1** in the reverse direction of the vibrational mode corresponding to the imaginary frequency was solved by the IRC calculation. The reactant **A1** was obtained through geometry optimization starting from the last point of the IRC calculation. The distance between Lys73Nζ and Ser130Oγ was 2.89 Å. Ha−Lys73Nζ and Ha−Ser130Oγ distances were 1.04 and 1.91 Å, respectively. The O_{C3}−Ser130Oγ distance was 2.61 Å. Hb−Ser130Oγ and Hb−O_{C3} distances were 1.01 and 1.64 Å, respectively. The structure of **A1** was almost the same as that shown in Figure 1b, which is the active site structure in the MD-derived AEI. To obtain the product of this reaction, the steepest reaction path from **TSA1** in the forward direction of the vibrational mode corresponding to the imaginary frequency was solved by the IRC calculation. The product **A2** was obtained through geometry optimization starting from the last point of the IRC calculation. The distance between Lys73Nζ and Ser130Oγ was 2.76 Å. Ha−Lys73Nζ and Ha−Ser130Oγ distances were 1.80 and 1.00 Å, respectively. The O_{C3}−Ser130Oγ distance was 2.65 Å. Hb−Ser130Oγ and H−O_{C3} distances were 1.69 and 1.00 Å, respectively. The distance between Glu166Oϵ and Lys73Nζ was 3.11 Å. This distance was longer than that in the reactant **A1** (2.74 Å). It is particularly notable that this double-PT reaction lengthened the distance between Glu166Oϵ and Lys73Nζ. The activation energy for this first reaction was calculated to be 7.9 kcal/mol.

3.1.2. Second Elementary Reaction. TI would be formed by an assistance of Glu166 working as a general base catalyst.

SCHEME 2

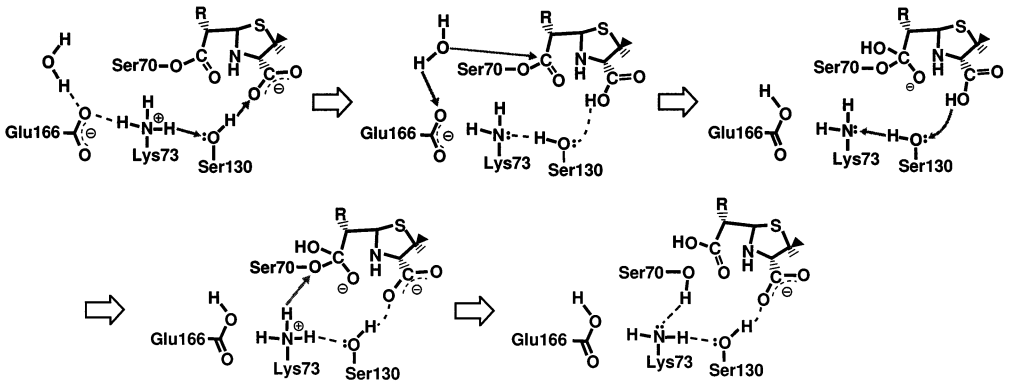

The transition state of the reaction **TSA2** was determined by the geometry optimization. The vibrational analysis indicated that there appeared only one normal vibrational mode with an imaginary frequency. In the largest atomic displacement of the vibrational mode, Ow approached the carbonyl carbon of the pen G adduct (C7), and Hw approached Glu166Oϵ in the second largest one. The distance between Ow and Glu166Oϵ was 2.50 Å. Hw−Glu166Oϵ and Hw−Ow distances were 1.07 and 1.47 Å, respectively. The Ow−C7 distance was 1.75 Å. To confirm that the reactant obtained from **TSA2** is identical with the product of the first elementary reaction **A2**, the steepest reaction path from **TSA2** in the reverse direction was solved by the IRC calculation. Furthermore, the structure of the reactant was completely determined by performing geometry optimization from the last point of the IRC calculation. These computations indicated that the reactant structure is identical with **A2**. The distance between Ow and Glu166Oϵ was 2.68 Å. Hw−Glu166Oϵ and Hw−Ow distances were 1.68 and 1.00 Å, respectively. According to these interatomic distances,**Wat** was held by Glu166. The Ow−C7 distance was 3.12 Å. To obtain the product of the second elementary reaction, the steepest reaction path from **TSA2** in the forward direction was solved by the IRC calculation. The product **A3** was obtained by geometry optimization starting from the last point of the IRC calculation. The distance between Ow and Glu166Oϵ was 2.62 Å. Hw−Glu166Oϵ and Hw−Ow distances were 1.01 and 1.68 Å, respectively. It was found that Ow was bound to C7 because the Ow−C7 distance was 1.57 Å. This means that the TI formation was completed in **A3**. The activation energy for this reaction was found to be 24.6 kcal/mol, which is the highest value in the deacylation reaction.

From the obtained mechanisms of the first and second elementary reactions, we could give a hypothesis that the reduction of ionic interaction between Glu166Oϵ and Lys73Nζ enhances general base activity of Glu166, and the reduction is caused by the deprotonation of Lys73. As described in section 3.1.1, it has been confirmed that the deprotonation of Lys73 is induced by the C3-carboxyl group in the substrate pen G. Therefore, this mechanism can be regarded as SAC.

3.1.3. Third Elementary Reaction. For detachment of the degraded substrate from the active site, it is necessary to donate a proton to Ser70Oγ to cleave the C7−Ser70Oγ bond. The catalytic residue which plays this role has been presumed to be Glu166.[8,11] This mechanism is depicted in Scheme 1I. According to the structure of **A3**, however, the distance between Glu166Oϵ and Ser70Oγ is too far for direct proton migration to occur (4.07 Å). Another mechanism that a proton migrates from Glu166Oϵ to Ser70Oγ via a water molecule located between Glu166Oϵ and Ser70Oγ has been also proposed.[9,13,20,21] This reaction is depicted in Scheme 1II. However,no water molecule was observed between Glu166Oϵ and Ser70Oγ during the MD calculation of this study. Judging from the facts above, Glu166 was not considered to be a candidate for the catalytic residue. For these reasons, the two hypothetical mechanism above might be incorrect. Lys73Nζ−Ser70Oγ and Hc−Ser70Oγ distances in **A3** were 2.71 and 1.87 Å, respectively. This probable mechanism, however, requires the protonated amino group of Lys73. Hence, it is necessary to reprotonate the Lys73 because the amino group was in neutral state in **A3**. We speculated that Ha migrates from Ser130Oγ to Lys73Nζ because a lone pair of Lys73Nζ was oriented toward Ha. Hence, the probable reaction mechanism of the reprotonation of Lys73 would be a concerted double-PT from O_{C3} to Ser130Oγ and from Ser130Oγ to Lys73Nζ.

The transition state of this reaction **TSA3** was determined using geometry optimization. The normal vibrational analysis suggested that there appeared only one normal vibrational mode with an imaginary frequency. In the largest atomic displacement, Ha moved from the Ser130Oγ to Lys73Nζ, and Hb moved from O_{C3} to Ser130Oγ in the second largest one. The distance between O_{C3}−Ser130Oγ was 2.44 Å. Hb−Ser130Oγ and Hb−O_{C3} distances were 1.33 and 1.15 Å, respectively. The Lys73Nζ−Ser130Oγ distance was 2.57 Å. Ha−Lys73Nζ and Ha−Ser130Oγ distances were 1.17 and 1.42 Å respectively. The steepest reaction path from **TSA3** to the reverse direction was solved by the IRC calculation to check if the reactant obtained from **TSA3** agreed with the product of the second elementary reaction. The reactant structure **A3′** was obtained by the geometry optimization starting from the last point of the IRC calculation. **A3′** was almost identical with **A3**.[60] In the **A3′**, the distance between O_{C3} and Ser130Oγ was 2.64 Å. Hb−Ser130Oγ and Hb−O_{C3} distances were 1.69 and 1.00 Å, respectively. The Lys73Nζ−Ser130Oγ distance was 2.70 Å. Ha−Lys73Nζ and Ha−Ser130Oγ distances were 1.74 and 1.02 Å, respectively. The steepest reaction path from **TSA3** to the forward direction was solved by the IRC calculation to obtain the product of this elementary reaction. The product **A4** was obtained by the geometry optimization starting from the last point of the IRC calculation. The distance between O_{C3} and Ser130Oγ was 2.64 Å. Hb−Ser130Oγ and Hb−O_{C3} distances were 1.01 and 1.71 Å, respectively. The Lys73Nζ−Ser130Oγ distance was 2.67 Å. Ha−Lys73Nζ and Ha−Ser130Oγ distances were 1.06 and 1.64 Å, respectively. Furthermore, the distance between Lys73Nζ and Ser70Oγ was 2.60 Å. Hc−Lys73Nζ and Hc−Ser70Oγ distances were 1.05 and 1.79 Å, respectively. It was found that **A4** is ready for the proton migration from Lys73Nζ to Ser70Oγ. The activation energy for this reaction was calculated to be 9.0 kcal/mol.

SCHEME 3

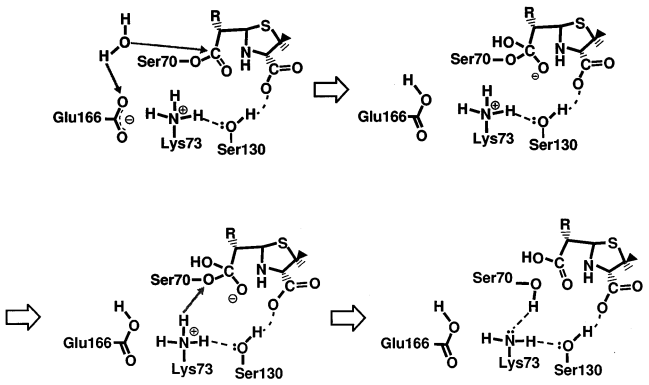

3.1.4. Fourth Elementary Reaction. The reaction mechanism of the detachment of the degraded substrate would be a process that the C7−Ser70Oγ bond is cloven in concert with the single proton migration from Lys73Nζ to Ser70Oγ. The transition state of this reaction **TSA4** was determined by geometry optimization. The vibrational analysis indicated an appearance of only one normal vibrational mode with an imaginary frequency. In the largest atomic displacement, Hc approached Ser70Oγ, and C7 was separated from Ser70Oγ in the second largest one. The distance between Lys73Nζ and Ser70Oγ was 2.57 Å. Hc−Lys73Nζ and Hc−Ser70Oγ distances were 1.58 and 1.04 Å, respectively. The C7−Ser70Oγ distance was 1.82 Å. The steepest reaction path from **TSA4** in the reverse direction was solved by the IRC calculation, and the reactant was obtained by the geometry optimization starting from the last point of the IRC calculation. The structure of the reactant was confirmed to be same as the product of the third elementary reaction **A4**. The distance between C7 and Ser70Oγ was 1.53 Å in **A4**. The steepest reaction path from **TSA4** in the forward direction was solved by the IRC calculation to obtain the product. The product **S5** was determined by the geometry optimization starting from the last point of the IRC calculation. The distance between Lys73Nζ and Ser70Oγ was 2.57 Å. Hc−Lys73Nζ and Hc−Ser70Oγ distances were 1.60 and 1.03 Å, respectively. Because the distance between C7 and Ser70Oγ was 1.85 Å, the C7−Ser70Oγ bond was dissociated. The activation energy for this reaction was found to be 3.6 kcal/mol.

3.2. Substrate-Independent Mechanism. If the C3-carboxyl group does not participate in the deacylation step, the mechanism would be based on a simple ester bond cleavage. First, the TI is formed by the nucleophillic attack on the C7. Second, the C7−Ser70Oγ bond is dissociated in concert with a single proton migration from Lys73Nζ to Ser70Oγ. This mechanism was summarized in Scheme 3. The potential energy curve of this deacylation path was successfully determined as shown in Figure 5. The TS structures obtained are shown in Figure 6. Structures of energy minima on this reaction path are shown in Figure 7. Atomic distances in the minima are listed in Table 2. The structure of the transition state **TSB1** for the TI formation was determined by the geometry optimization from the initial model compound. The atomic locations important in TI formation of **TSB1** were similar to those in **TSA2**. Reactant **B1** and product **B2** were obtained from **TSB1**. It should be noted that the potential energy and the geometry of **B1** were completely identical with those of **A1**. The activation energy for this TI formation was found to be 26.8 kcal/mol. The C7−Ser70Oγ bond cleavage mechanism was determined in a similar manner. In the geometry of **B2**, the proton migration from Lys73Nζ to Ser70Oγ was considered to be possible because the distance between Lys73Nζ and Ser70Oγ was 2.61 Å. The TS of the proton migration from Lys73Nζ to Ser70Oγ(**TSB2**) was obtained from **B2**. The reactant and the product of this elementary reaction were obtained from **TSB2**. The reactant was almost equal to the product of the TI formation **B2**. In the product **B3**, the distance between C7 and Ser70Oγ was 1.91 Å. This means that the deacylation path was completed. The activation energy computed was 2.4 kcal/mol.

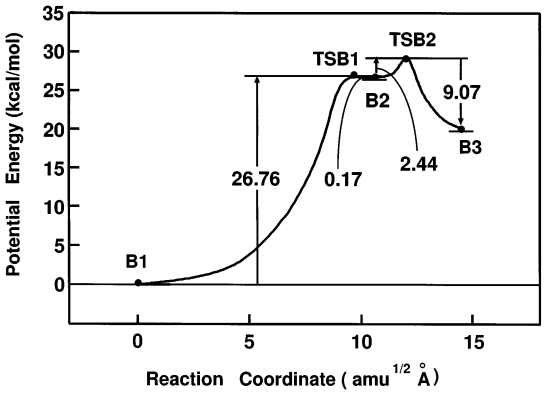

Figure 5. Potential energy profile of substrate-independent path.

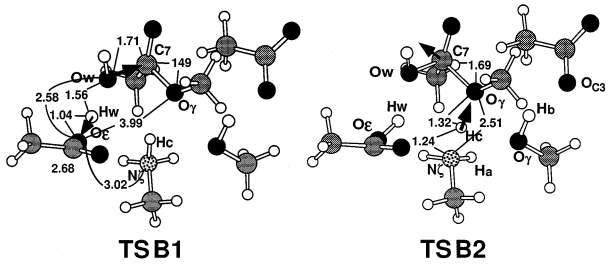

Figure 6. TS structures on substrate-independent path.

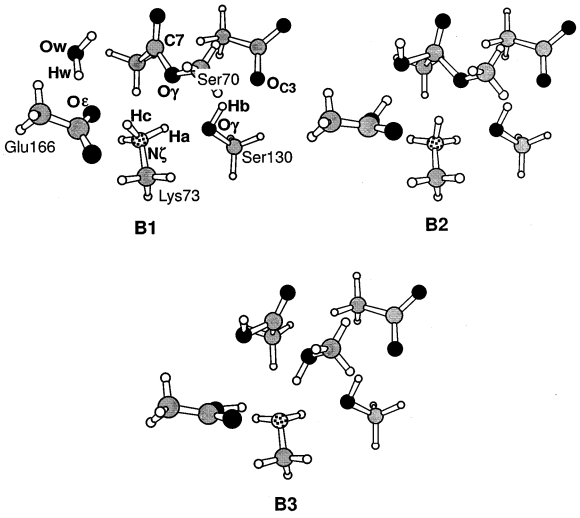

Figure 7. Structures of energy minima on substrate-independent path.

4. Discussion

4.1. Substrate Assisted Catalysis and the Role of the C3-Carboxyl Group. Substrate-assisted catalysis (SAC) is an enzymatic reaction which is accelerated by a functional group of a substare. It has been proposed that SAC can be observed in the catalytic mechanism of many different types of enzymes.[61] The deacylation mechanism described in section 3.1 depends on C3-carboxyl group of the substrare. Hence, this deacylation mechanism seems to be SAC. To figure out whether the C3-carboxyl group accelerates the deacylation reaction or not, we

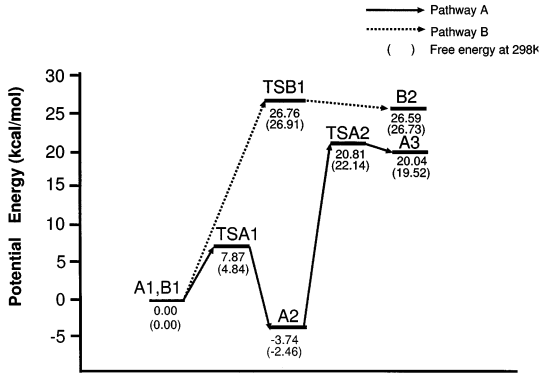

Figure 8. Potential energy diagrams for the TI formation in pathways A and B. Values in parentheses indicate the relative free energy at 298 K.

TABLE 2: Important Atomic Distances for the Energy Minima along Substrate-Independent Path

atomic distance(Å)	B1	B2	B3
C7−Ow	3.10	1.59	1.39
C7−Ser70Oγ	1.37	1.52	1.91
Ow−Glu166Oϵ	2.74	2.66	3.06
Ser70Oγ−Glu166Oϵ	3.74	4.00	4.10
Ser70Oγ−Lys73Nζ	2.67	2.61	2.60
Lys73Nζ−Glu166Oϵ	2.73	3.05	2.89
Hc−Ser70Oγ	1.08	1.05	1.68
Hw−Ow	2.59	1.77	1.00
Hw−Glu166Oϵ	0.99	1.67	2.74
Hw−Ser70Oγ	1.72	1.01	0.98
Hc−Ser70Oγ	3.59	3.14	3.24

also examined another deacylation mechanism without the C3-carboxyl group. To distinguish the two deacylation pathways, in this section, the deacylation path described in section 3.1 is referred to as pathway A and the another deacylation path in section 3.2 is referred to as pathway B. The potential energy diagram of TI formation mechanisms in pathway A and B was depicted in Figure 8. It clearly shows that pathway A takes a lower energy surface compared with pathway B. Further, the activation energy for the TI formation in pathway A(**A2** → **TSA2**; 24.6kcal/mol) was smaller than that of TI formation in pathway B(**B1** → **TSB1**; 26.8kcal/mol). The activation energy difference was 2.2 kcal/mol. Therefore, pathway A is energetically more favorable compared to pathway B. The reduction of potential barrier height at the TI formation is important for the efficiency of the catalysis because the TI formation has the highest energy barrier in the deacylation reaction. Accordingly, we can safely conclude that the C3-carboxyl group accelerated the deacylation reaction. To take thermodynamical correction into account, free energy calculations based on vibrational frequency were performed on each stationary point for the TI formation in the two pathways. In this computation, temperature used was 298 K. The result is shown as a value in parentheses of Figure 6. The changes in the free energy from **A2** to **TSA2** was found to be 24.6 kcal/mol, and from **B1** to **TSB1**, it was 26.9 kcal/mol. Hence, also on the free energy surface, TI formation in pathway A was more favorable. To examine the cause of the reduction of the energy barrier, the geometry of the reactant of pathway A (**A2**) was compared with that of pathway B (**B1**). It was found from the comparison that the Glu166Oϵ−Lys73Nζ distance in **B1** (2.73 Å) was shorter than that in **A1** (3.11 Å). Accordingly, it means that an ionic interaction between Glu166Oϵ and Lys73Nζ in **B1** is tighter compared to that in **A1**. It was considered that the general base activity of Glu166 in **B1** decreased because of the protonation of Lys73. On the other hand, in **A2**, that of Glu166 did not decrease so much because the Lys73 was already deprotonated. This might be the reason the TI formation of pathway A requires less activation energy compared with that of pathway B. We have found that the deprotonation of Lys73 was induced by the C3-carboxyl group of the substrate. Therefore, it can be concluded that the deacylation by pathway A is SAC.

SAC in the catalysis of class A β-lactamase has been reported at several studies. Strynadka et al. proposed a reaction mechanism in which the nitrogen in the five-membered ring of the substrate abstracted a proton of the amino group of the Lys73 side chain via the hydroxyl group of Ser130.[11] Ishiguro and Imajo suggested a mechanism in which the C3-carboxyl group abstracted the proton of Lys73 via Ser130.[22] Recently, Diáz et al. proposed a mechanism that the C3-carboxyl group abstracted a proton of the hydroxyl group of Ser70 via Ser130.[62] It should be noted that these SAC mechanisms are considered to induce the acylation step. Our results indicated that SAC was not only in the acylation step but also in the deacylation step. The SAC found in this study was similar to the mechanism proposed by Ishiguro and Imajo because the deprotonation of Lys73 is induced by the C3-carboxyl group in both Ishiguro's mechanism and ours. Furthermore, Zawadzke et al. suggested that the pK_a of Lys73 was dramatically reduced upon the substrate binding,[63] which is also compatible with our mechanism.The substrate molecule examined in this study was only pen G. However, our SAC may be applied to the enzymatic hydrolysis of other penicillins because penicillins generally have a C3-carboxyl group in their five-membered ring. It is interesting that several β-lactams that have no functional group at C3 work as β-lactamase inhibitors.[64] This suggests that the inhibition ability of the compounds arises from an absence of the C3-carboxyl group. As is well-known, cepharosporin antibiotics have a carboxyl group at C4. The role of the C4-carboxyl group seems to be similar to that of the C3-carboxyl group of the penicillins. According to the QM calculation study by Vaterro et al., however, the orientation of the C4-carboxyl group differed from that of the C3-carboxyl group of penicillins.[40] Moreover,the structural analysis of the cepharoridine-acylated double mutant (Glu166Asp:Asn170Gln) showed that the C4-carboxyl group made a weak hydrogen bond with Ser130Oγ (the C4-carboxyl oxgen-Ser130Oγ distance was found to be 3.78 Å).[65] From the findings above, the C4-carboxyl group does not seems to be appropriate for the proton abstractor from the hydroxyl group of Ser130. Hence, the reaction path shown in section 3.1 would be impossible in the deacylation of cephalosporins because C4-carboxyl group cannot participate in the deacylation process. This would be the reason cepharosporins show the better resistance to the β-lactam compound compared with penicillins. An experimental study by Christensen et al. has shown that the deacylation rate of cephalosporin(nitrocefin) is considerably smaller than that of pen G.[66] This result is well compatible with our suggestion described above.

4.2. Role of Lys73. It was reported that the deacylation ability of the Lys73 mutant was lower compared with that of the WTE, which indicated that Lys73 had some role in the deacylation.[4,67] In this study, our calculations demonstrated that the role of Lys73 was the proton donor to Ser70Oγ in the detachment of the degraded substrate from the active site of the enzyme. Accordingly, it is concluded that mechanism III in Scheme 1 is the most reasonable mechanism for the detachment of substrate. The hypothetical mechanism involving Glu166, I and II, should be rejected from the appearance of the structure of **A3**. The details about this mechanism have already been given in the

section 3.1.3. It is notable that the deacylation is not proceeded only by Glu166 but that Lys73 also participates in the reaction.

4.3. Role of Ser130. It was found that Ser130 made a bridge between Lys73 and the C3-carboxyl group. It has been reported that Ser130 mutants represent less substrate affinity.[68,69] The several structural studies on the AEI analogues indicated that Ser130 made a hydrogen bond with the carboxyl group.[11,70−72] From these experimental findings, the function of Ser130 was considered to be bind substrate. Dietz et al. suggested that Ser130 did not only take part in the substrate binding but also the enzymatic catalysis.[62] The present study suggested that the Ser130 was a residue assisting the substrate binding and the deacylation mechanism. Therefore, our study is consisted with the previous studies.

4.4. TI Formation Mechanism and the Effect of Amino Acid Residues around the Active Site. The results of this study found that the function of Glu166 in the deacylation was a general base catalyst for the TI formation reaction. The TI formation mechanism obtained in this work is consistent with several experimental studies in which the deacylation ability of Glu166 mutant was shown to be extremely impaired relative to that of WTE.[4,8,10,12−14] In our study, the activation energy for the TI formation in pathway A was 24.6 kcal/mol, and the reaction appeared to be the rate-determining step of the deacylation step. Wladkowski et al. have found that the rate-determing step in the acylation half was TI formation, and the activation energy was calculated to be 25.9 kcal/mol at the B3LYP/6-31+G* level.[36] Thus, some theoretical investigations are also consistent with our results. Pitarch et al. clarified the mechanism of the water molecule inducing nonenzymatic hydrolysis of a β-lactam compound, executing ab initio MO calculations at the HF/6-31G* level. They suggested that the rate-determing step in the nonenzymatic hydrolysis was TI formation, and the activation energy of the reaction was evaluated to be 53.77 kcal/mol.[73] The TI formation in the present study is energetically more favorable compared with the nonenzymatic TI formation. This demonstrates the catalytic efficiency of the enzyme.

The energy barrier height for the TI formation was computed to be 24.6 kcal/mol. It seemed to be somewhat high for an enzymatic reaction. Furthermore, the stabilization energy from **TSA2** to **A3** was only 0.77 kcal/mol. In our previous study, the amino acid residues around the active site were suggested to have a good potential to reduce the activation energy.[2] Hence, it was considered that this barrier height problem arises from the neglect of residues around the active site. To take the effects of the residues into computation, we constructed two extended models from the MD-derived AEI. One extended model involves the whole side chain of the four catalytic residues (Ser70, Lys73, Ser130, and Glu166) and six residues locating within 5 Å from Ser70Oγ (Ala69, Thr71, Asn132, Ser235, Gly236, and Gln237). We referred to this model as the "extended model I". Another large model involves the whole side chain of the four catalytic residues and seven residues that are highly conserved in various type of class A β-lactamase and located near the catalytic site (Asp131, Asn132, Asn170, Lys234, Ser235, Gly236, and Gln237). This model is referred to as the "extended model II". The water molecule involved in the two extended models is only **Wat**, as shown in Figure 1a because even the closest water molecule from **Wat** did not interact with the active site. The two large models contain the full structure of the pen G adduct. A total of 24 core atoms are included in both of the extended models and the model compound that is shown in Figure 1b. The positions of these 24 atoms in the extended models were changed to match those in the stationary points appeared on the pathway A, i.e., **A2**, **TSA2**, and **A3** in Figure 3. Because the atoms marked by asterisks in Figure 1b were fixed through computation on the deacylation mechanisms, the positions of these atoms are equal to those shown by asterisks in Figure S1 in the Supporting Information. The extended models I and II are shown in Figures 1.S1 and 1.S2, respectively. A2-I, TSA2-I, and A3-I are the extended model I for **A2**, **TSA2**, and **A3**, respectively. Similary, A2-II, TSA2-II, and A3-II are the extended model II for these stationary points. For these extended models,only potential energy calculation were performed at B3LYP level using 6-31G** basis set because of the limitation of computational facility. The result is shown in Figure S3 of the Supporting Information. The activation energy for TI formation was evaluated to be 6.5 kcal/mol (**A2I → TSA2I**) when the extended model I was used and 4.3 kcal/mol (**A2II → TSA2II**) in the extended model II. These values were obviously smaller than that obtained using the small model compound (24.6 kcal/mol). Furthermore, the stabilization energy from the TS structure to the TI was found to be 3.1 kcal/mol (**TSA2II → A3II**) in the extended model I and 4.2 kcal/mol (**TSA2II → A3II**) in the extended model II. Hence, the amino acid residues around the active site contributed to the reduction of the activation energy for TI formation and the stabilization of TI. It should be noted that these extended models involve the oxy-anion hole which is composed of two main chains of Ser70 and Gln237. Wladkowski et al. demonstrated that the polarization of the carbonyl group of the substrate induced by the oxy-anion hole reduced the activation energy of TI formation in the acylation step.[36] We could confirm the same polarization effect in the extended models. Therefore, it was considered that the barrier height reduction mainly results from involving the oxy-anion hole.

5. Conclusion

The DFT quantum chemical calculations were performed to clarify the reaction mechanism of the deacylation in the catalysis of class A β-lactamase. Two pathways for the deacylation were examined. One pathway proceeds via four elementary reactions. This pathway is remarkably assisted by the C3-carboxyl group of the substrate. Another reaction pathway consists of two elementary reactions. The TI formation in the C3-carboxyl group-assisted former pathway is energetically more favorable compared to that in the latter pathway. Therefore, the deacylation mechanism is demonstrated to be the SAC. The catalytic role of the C3-carboxyl group is the deprotonation of Lys73 via Ser130. The deprotonation of Lys73 could increase the general base activity of Glu166. The catalytic role of Lys73 in the deacylation is the proton donor to Ser70, which induces the detachment of the degraded substrate from the active site of the enzyme.

Acknowledgment. The authors thanks the Computer Center for the Institute of Molecular Science, for the use of the IBM SP2 computer.The computations were also carried out by the DRIA System at the Faculty of Pharmaceutical Sciences, Chiba University.

Supporting Information Available: Structures (Figures S1 and S2) and energy diagrams (Figure S3) of the extended models I and II. This material is available free of charge via the Internet at http://pubs.acs.org.

References and Notes

(1) Matagne, A.; Frère, J.-M. *Biochim. Biophys. Acta.* **1995**, *1246*, 109−127.

(2) Hata, M.; Fujii, Y.; Ishii, M.; Hoshino, T.; Tsuda, M. *Chem. Pharm. Bull.* **2000**, *48*, 447−453.
(3) Hertzberg, O.; Moult, J. *Science* **1987**, *236*, 694−701.
(4) Gibson, R. M.; Christensen, H.; Waley, S. G. *Biochem. J.* **1990**, *272*, 613−619.
(5) Knox, J. R.; Moews, P. C. *J. Mol. Biol.* **1991**, *220*, 435−455.
(6) Hertzberg, O.; Kapadia, G.; Blanco, B.; Smith, T. S.; Coluson, A. *Biochemistry* **1991**, *30*, 9503−9509.
(7) Hertzberg, O. *J. Mol. Biol.* **1991**, *217*, 701−719.
(8) Adachi, H.; Ohta, T.; Matsuzawa, H. *J. Biol. Chem.* **1991**, *266*, 3186−3191.
(9) Lamotte-Brasseur, J.; Jacob-Dubuisson, F.; Dive, G.; Frère, J.-M.; Ghuysen, J.-M. *Biochem. J.* **1991**, *279*, 213−221.
(10) Escobar, W. A.; Tan, A. K.; Fink, A. L. *Biochemistry* **1991**, *30*, 10783−10787.
(11) Strynadka, N. C. J.; Adachi, H.; Jensen, S. E.; Johns, K.; Sielecki, A.; Betzel, C.; Sutoh, K.; James, M. N. G. *Nature* **1992**, *359*, 700−705.
(12) Knox, J. R.; Moews, P. C.; Escobar, W. A.; Fink, A. L. *Protein Eng.* **1993**, *6*, 11−18.
(13) Escobar, W. A.; Tan, A. K.; Lewis, E. R.; Fink, A. L. *Biochemistry* **1994**, *33*, 7619−7626.
(14) Leung, Y-. C.; Robinson, C. V.; Aplin, R. T.; Waley, S. G. *Biochem. J.* **1994**, *299*, 671−678.
(15) Swarén, P.; Maveyraud, L.; Guillet, V.; Masson, J.-M.; Mourey, L.; Samama, J.-P. *Structure* **1995**, *3*, 603−613.
(16) Vijayakumar, S.; Ravishanker, G.; Pratt, R. F.; Beveridge, D. L. *J. Am. Chem. Soc.* **1995**, *117*, 1722−1730.
(17) Chen, C. C. H.; Hertzberg, O. *Protein Eng.* **1999**, *12*, 573−579.
(18) Raquet, X.; Lounnas, V.; Lamotte-Brasseur, J.; Frère, J. -M.; Wade, R. C.; *Biophys. J.* **1997**, *73*, 2416−2426.
(19) Lamotte-Brasseur, J.; Lounnas, V.; Raquet, X.; Wade, R. C. *Protein Sci.* **1999**, *8*, 404−409.
(20) Lamotte-Brasseur, J.; Jacob-Dubuisson, F.; Dive, G.; Frère, J. -M.; Ghuysen, J. -M. *Biochem. J.* **1992**, *282*, 189−195.
(21) Damblon, C.; Raquet, X.; Lian, L. Y.; Lamotte-brasseur, J.; Fonzè, E.; Charlier, P.; Roberts, G. C. K.; Frère, J. M. *Proc. Natl. Acad. Sci. U.S.A.* **1996**, *93*, 1747−1752.
(22) Ishiguro, M.; Imajo, S. *J. Med. Chem.* **1996**, *39*, 2207−2218.
(23) Blow, D. M.; Birktoft, J. J.; Hartley, B. S. *Nature* **1969**, *221*, 337−340.
(24) Umeyama, H.; Nakagawa, S.; Kudo T. *Chem. Pharm. Bull.* **1980**, *28*, 1342−1344.
(25) Umeyama, H.; Nakagawa, S.; Kudo, T. *J. Mol. Biol.* **1981**, *150*, 409−421.
(26) Kollman, P. A.; Hayes, D. M. *J. Am. Chem. Soc.* **1981**, *103*, 2955−2961.
(27) Tapia, O.; Sussman, F.; Poulain, E. *J. Theor. Biol.* **1978**, *71*, 49−72.
(28) Longo, E.; Stamato, F. M. L. G.; Ferreira, R.; Tapia, O. *J. Theor. Biol.* **1985**, *112*, 783−798.
(29) Warshel, A.; Russell, S. *J. Am. Chem. Soc.* **1986**, *108*, 6569−6579.
(30) Warshel, A.; Naray-Szabo, G.; Sussman, F.; Hwang, J. −K. *Biochemistry* **1989**, *28*, 3629−3637.
(31) Onsager, H. B. *J. Am. Chem. Soc.* **1936**, *58*, 1486−1493.
(32) Tapia, O.; Goscinski, O. *Mol. Phys.* **1975**, *29*, 1653−1661.
(33) Wong, M. W.; Frisch, M. J.; Wiberg, K. B. *J. Am. Chem. Soc.* **1991**, *113*, 4776−4782.
(34) Tomasi, J.; Persico, M. *Chem. Rev.* **1994**, *94*, 2027−2094.
(35) Solà, M.; Lledós, A.; Duran, M.; Bertráin, J. *J. Am. Chem. Soc.* **1992**, *114*, 869−877.
(36) Wladkowski, B. D.; Chenoweth, S. A.; Sanders, J. N.; Krauss, M.; Stevens, W. J. *J. Am. Chem. Soc.* **1997**, *119*, 6423−6431.
(37) Hata, M.; Hirano, Y.; Hoshino, T.; Tsuda, M. *J. Am. Chem. Soc.* **2001**, *123*, 6410−6416.
(38) Murata, K.; Fujii, Y.; Enomoto, N.; Hoshino, T.; Tsuda, M. *Biophys. J.* **2000**, *79*, 982−991.
(39) Laws, A. P.; Page, M. I. *J. Chem. Soc., Perkin. Trans. 2* **1989**, 1577−1581.
(40) Varetto, L.; De Meester, F.; Monnaie, D.; Marchand-Brynaert, J.; Dive, G.; Jacob, F.; Frère, J. -M. *Biochem. J.* **1991**, *278*, 801−807.
(41) Chen, C. C.; Hertzberg, O. *J. Mol. Biol.* **1992**, *224*, 1103−1113.
(42) Abola, E. E.; Bernstein, F. C.; Bryant, S. H.; Koetzle, T. F.; Weng, J. Protein Data Bank. In *Crystallographic Databases-Information Content, Software Systems, Scientific Applications*; Allen, F. H., Bergerhoff, G., Sievers, R., Eds.; Data Commission of the International Union of Crystallography: Cambridge/Chester, U.K., 1987; pp 107−132.
(43) Abola, E. E.; Manning, N. O.; Prilusky, J.; Stampf, D. R.; Sussman, J. L. *J. Res. Natl. Inst. Stand. Technol.* **1996**, *101*, 231−241.
(44) Pearlman, D. A.; Case, D. A.; Caldwell, J. W.; Ross, W. S.; Cheatham, T. E. III.; Ferguson, D. M.; Seibel, G. L.; Singh, U. C.; Weiner, P. K.; Kollman, P. A. *AMBER4.1*; University of California: San Francisco, CA, 1995.
(45) Weiner, S. J.; Kollman, P. A.; Case, D. A.; Singh, U. C.; Ghio, C.; Alagona, G.; Profeta, S., Jr.; Weiner, P. J. *J. Am. Chem. Soc.* **1984**, *106*, 765−784.
(46) Weiner, S. J.; Kollman, P. A.; Nguyen, D. T.; Case, D. A. *J. Comput. Chem.* **1986**, *7*, 230−252.
(47) Stewart J. J. P. *J. Comput. Chem.* **1989**, *10*, 221−264.
(48) Jorgensen, W. L.; Chandrasekhar, J.; Madura, J. D. *J. Chem. Phys.* **1983**, *79*, 926−935.
(49) Ryckaert, J. P.; Ciccotti, G.; Berendsen, H. J. C. *J. Comput. Phys.* **1977**, *23*, 327−341.
(50) Toyoda, S.; Miyagawa, H.; Kitamura, K.; Amisaki, T.; Hashimoto, E.; Ikeda, H.; Kusumi, A.; Miyagawa, N. *J. Comput. Chem.* **1999**, *20*, 185−199.
(51) Becke, A. D. *J. Chem. Phys.* **1993**, *98*, 5648−5652
(52) Lee, C.; Yang, W.; Parr, R. G. *Phys. Rev. B* **1988**, *37*, 785−789.
(53) Schlegel, H. B. *J. Comput. Chem.* **1981**, *3*, 214−218.
(54) Fukui, K. *Acc. Chem. Res.* **1981**, *14*, 363−368.
(55) Murphy, B. P.; Pratt, R. F. *Biochem. J* **1988**, *256*, 669−672.
(56) Antosiewicz, J.; McCammon, J. A.; Gilson, M. K. *J. Mol. Biol.* **1994**, *238*, 415−436.
(57) Antosiewicz, J.; McCammon, J. A.; Gilson, M. K. *Biochemistry* **1996**, *35*, 7819−7833.
(58) Sham, Y. Y.; Muegge, I.; Warshel, A. *Biophys. J.* **1996**, *74*, 1744−1753.
(59) Frisch, M. J.; Trucks, G. W.; Schlegel, H. B.; Scuseria, G. E.; Robb, M. A.; Cheeseman, J. R.; Zakrzewski, V. G.; Montgomery, J. A., Jr.; Stratmann, R. E.; Burant, J. C.; Dapprich, S.; Millam, J. M.; Daniels, A. D.; Kudin, K. N.; Strain, M. C.; Farkas, O.; Tomasi, J.; Barone, V.; Cossi, M.; Cammi, R.; Mennucci, B.; Pomelli, C.; Adamo, C.; Clifford, S.; Ochterski, J.; Petersson, G. A.; Ayala, P. Y.; Cui, Q.; Morokuma, K.; Malick, D. K.; Rabuck, A. D.; Raghavachari, K.; Foresman, J. B.; Cioslowski, J.; Ortiz, J. V.; Stefanov, B. B.; Liu, G.; Liashenko, A.; Piskorz, P.; Komaromi, I.; Gomperts, R.; Martin, R. L.; Fox, D. J.; Keith, T.; Al-Laham, M. A.; Peng, C. Y.; Nanayakkara, A.; Gonzalez, C.; Challacombe, M.; Gill, P. M. W.; Johnson, B. G.; Chen, W.; Wong, M. W.; Andres, J. L.; Head-Gordon, M.; Replogle, E. S.; Pople, J. A. *Gaussian 98*, revision A.7; Gaussian, Inc.: Pittsburgh, PA, 1998.
(60) The structure of **A3′** did not completely correspond to that of **A3″**. However, the strucutral difference between **A3′** and **A3** was only a conformation of carboxyl group of Glu166. Further, Glu166 did not participiate in the 3rd elementary reaction. It should be also noted that the potential energy of **A3′** was almost same as that of **A3** (the energy difference was only 0.3 kcal/mol). Therefore, we assumed that **A3** and **A3′** were indentical in the terms of reaction mechanism.
(61) Dall'acqua, W.; Carter, P. *Protein Sci.* **2000**, *9*, 1−9.
(62) Diáz, N.; Suárez, D.; Sordo, T. L.; Merz, K.-M., Jr. *J. Phys. Chem. B* **2001**, *105*, 11302−11313.
(63) Zawadzke, L. E.; Chen, C. C. H.; Banerjee, S.; Li, Z.; Wäsch, S.; Kapadia, G.; Moult, J.; Hertzberg, O. *Biochemistry* **1996**, *35*, 16475−16482.
(64) Wanning, M.; Zähner, H.; Krone, B.; Zeeck, A. *Tetrahedon Lett.* **1981**, *22*, 2539−2540.
(65) Chen, C. C. H.; Hertzberg, O. *Biochemistry* **2001**, *40*, 2351−2358.
(66) Christensen, H.; Martin, M. T.; Waley S. G. *Biochem. J.* **1990**, *266*, 853−861.
(67) Lietz, E. J.; Truher, H.; Kahn, D.; Hokenson, M. J.; Fink, A. L. *Biochemistry* **2000**, *39*, 4971−4981.
(68) Jacob, F.; Joris, B.; Lepage, S.; Dusart, J.; Frère, J.-M. *Biochem. J* **1990**, *271*, 399−406.
(69) Juteau, J.-M.; Billings, E.; Knox, J. R.; Levesque, R. C. *Protein Eng.* **1992**, *5*, 693−701.
(70) Maveyraud, L.; Massova, I.; Brick, C.; Miyashita, K.; Samama, J.-P.; Mobashery, S. *J. Am. Chem. Soc.* **1996**, *118*, 7435−7440.
(71) Mourey, L.; Miyashita, K.; Swarén, P.; Bulychev, A.; Samama, J.-P.; Mobashery, S. *J. Am. Chem. Soc.* **1998**, *120*, 9382−9383.
(72) Maveyraud, L.; Mourey, L.; Kotra, L. P.; Pedelacq, J.-D.; Guillet, V.; Mobashery, S.; Samama, J. −P. *J. Am. Chem. Soc.* **1998**, *120*, 9748−9752.
(73) Pitarch, J.; Ruiz-López, M. F.; Silla, E.; Pascual-Ahuir, J.-L.; Tuñón, I. *J. Am. Chem. Soc.* **1998**, *120*, 2146−2155.